



AQUILA OPTIMIZED NONLINEAR CONTROL FOR DC-DC BOOST CONVERTER WITH CONSTANT POWER LOAD

LOKESH DEVARAJAN¹, SENTHILSINGH CHELLATHURAI²

Keywords: Constant power loads; Aquila optimization algorithm; Super twisting algorithm; DC-DC Boost Converter and sliding mode controller.

Constant power loads (CPL) can be operated by tight-controlled power electronic converters, which have negative impedance and absorb continuous power. Constant power load creates instability in an open-loop system because of its negative incremental impedance. To tackle this problem, a discrete sliding-mode (AQO-DSM) nonlinear control technique has been proposed for a DC-DC boost converter fed CPL based on Aquila optimization. In this paper, the proposed AQO-DSM controllers provide the system stability during a steady state and maintain output voltage regardless of input voltage or CPL variations. In this case, the DSM controller of a DC-DC boost converter's characteristics are adjusted using the Aquila optimization method (AQO). The Lyapunov stability concept is utilized to assess the system's overall stability. Under various system operating conditions, an experimental study and simulation are carried out to validate the proposed controller. The existing methods, such as sliding mode controller (SMC), fuzzy-based SMC (F-SMC), and super twisting algorithm (STA)-based SMC strategies, are compared with a proposed plan to demonstrate the superiority of the proposed AQO-DSMC. Simulated and experimental results have shown that the AQO-DSMC achieves the fastest convergence, the smallest steady-state, settling time under loaded conditions, and consistent chatter reduction compared with all contrasted control methods.

1. INTRODUCTION

Microgrid (MG) use has increased dramatically in recent years due to environmental challenges such as inadequate fossil fuel supplies, emissions of gas, and worldwide climate change. Microgrids are becoming more popular for reasons including simplicity of control, absence of frequency and reactive power elements, and energy efficiency [1,2]. Despite these benefits, MG's most significant issue is stability, exacerbated by persistent power demands. Many components are made into MG, including power electronic converters, energy storage systems, and renewable energy sources [3,25]. Meanwhile, DC-DC converters are becoming more prevalent and crucial in microgrids because of their benefits in efficiency, flexibility, isolation, controllability, and so on. [4]. Electric cars and Constant Power Loads (CPL) in MG architectures also generate unique loads.

While the simultaneous impedance value is constantly positive in CPL behavior, its evolution is continuously negative. An increase or decrease in voltage is necessary for CPL to reach constant power. The negative impedance effect describes the phenomenon in this scenario, and negative impedance instability describes the system's instability [5,6]. The negative impedance characteristic of CPL behavior will cause the DC-DC converter to be unstable. As a result, improved control methods must be developed to reduce the impact of negative impedance on the DC-DC converter, provide a quick dynamic response, and ensure converter stability.

As a result, the CPL issue has caught the attention of many researchers looking for practical control approaches to avoid CPL instability difficulties. Furthermore, the disturbances caused by the DC source voltage and load current and changes in system parameters may result in a loss of system performance [7,26]. The system's stability is not assured because it may be entirely lost if significant limitation variation occurs in physical elements of the system under control utilizing classical controllers.

To resolve the issues previously mentioned, traditional methods that rely on conventional controllers may not be effective. The DC/DC converter's nonlinearity has been considered when developing nonlinear control techniques

[8,23]. To implement boost/buck converters with sliding mode control (SMC) are implemented [9]. Despite significant input voltage and load power variations, the system can stabilize over its entire operating range. In addition to model predictive control (MPC), other tools can be employed to moderate the adverse effects of CPLs [10,24]. Their implementation may be complex and costly, entail the use of many sensors, and reduce the efficiency of their systems by introducing passive elements.

This work offers a simple way to develop an Aquila optimization-based discrete sliding mode (AQO-DSM) controller for a source-side boost converter.

In this paper, the key contributions are summarized as follows.

- The proposed Aquila optimization-based discrete sliding mode (AQO-DSM) controller assures system stability and maintains that the output voltage remains consistent regardless of input voltage or CPL changes.
- Here, the Aquila optimization algorithm is employed to tune the parameters of a DSM controller of a boost converter. The system's stability is evaluated using the Lyapunov theory.

The organization of this paper is as follows: section 2 surveys recent relevant works. Section 3 describes the modeling of a DC-DC converter and system configuration. Section 4 presents the proposed AQO-DSM controller with a constant power load control strategy and stability analysis. Section 5 analyses the simulation and experimental setup of the proposed system. Section 6 describes the conclusion.

2. LITERATURE REVIEW

This section provides the recent related works of the various converter control strategies with constant power load in microgrid systems.

Marcillo, K.E.L. [11] presented a parametric control technique to create a fixed-order robust controller for reducing oscillations produced by a constant power demand in a DC multi-converter buck-buck system that ensures performance and stability throughout a preset uncertainty range. Wu gave a boost converter in a DC microgrid that uses

¹ Anna University, Chennai 600025 India. Correspondence address, E-mail: lokesh.d@sugunace.com

² Department of Computer Science and Engineering, Infant Jesus College of Engineering, Thoothukudi, Tamilnadu, 628851, India. E-mail: Principal@ijce.ac.in

the CPL an adaptive back-stepping SMC technique, J. *et al.* (2019) [12] to improve DC bus voltage stability. The composition assumes Brunovsky's canonical form, which is a linear structure. Its poor robustness is a drawback of this method.

Wang, J. [13] suggested an interval type-2 fuzzy system-based dynamic SMC solution to the robust voltage control of boost converters, which is dependent on the capacitor voltage and the target voltage. For cascaded DC/DC converters with an LC filter, Pang, S. [14] presented a modified damping assignment interconnection and passivity-based control. Due to its structure, the recommended technique is robust against external disturbances; conversely, the observer design is complex.

To stabilize a DC buck/boost converter with CPLs without making any assumptions or approximations, He, W. *et al.* (2019) [15] generated an adaptive energy shaping control (AESC) method. It involves rigorous stability investigation of converters with CPLs operating in discontinuous conduction mode and controller architecture. For distributed power supply in a DC microgrid, Xu, Q. [16] suggested a reliable droop-based controller with excellent signal stability. An observer of nonlinear disturbances estimates the interactions between individual DG interface converter subsystems and other DG interface converters.

Boukerdja, M. [17] presented a Golver Doyle optimization algorithm (GDOA) based source-side buck converter H_∞ controller; instabilities caused by the converter of load-side performance as a CPL can be prevented. Implementing this controller will reduce the implementation cost, and current measurement will not be used, which may have disadvantages. There can be no guarantee that these techniques will remain stable despite uncertainties. Azizi, A. [18] introduced Interlink converters, and consistent power demands are modeled using tiny signals. The suggested solution uses the control system's small-signal equivalent model of the CPL and IC units, as well as the dynamic model of the converter.

Kaplan, O. [19] proposed SMC based on a super twisting algorithm (STA) for a buck converter fed CPL in a cascade model. It has been calculated that utilizing STA-SMC would fulfill the stability criterion for converters fed CPL and robustly manage the output voltage. Nizami, T.K. [20] proposed a framework for tracking angular velocity in a step-down converter-powered permanent magnet DC motor unit, and a neuro-adaptive control strategy was proposed. The controller is based on the concept of backstepping and is composed of a Hermite neural network (HNN) with a fast single hidden layer module with on-board learning to compensate for the varying load torque.

3. MODELING OF A BOOST CONVERTER WITH CPL

Each source is linked to the microgrid by DC-DC converters. Rectifier/inverter interfaces are used to link DC microgrids to utility grids. In this situation, a DC microgrid will face challenges such as unbalanced power between loads and energy sources and voltage changes on the DC bus [21]. The structure of a proposed converter is depicted in Fig. 1. u denotes the duty cycle of the switch, load resistance (R), inductor (L), capacitor (C), freewheeling diode (D), controlled power switch (S), and V_o , V_{in} , i_L signify the average output voltage, input voltage, and inductor current, respectively.

When switch ON ($0 < t < dt$)

$$\begin{cases} i_L^* = \frac{V_{in}}{L} \\ V_0^* = -\frac{\theta V_0}{c} \end{cases} \quad (1)$$

When switching OFF ($dt < t < T$)

$$\begin{cases} i_L^* = \frac{V_{in}-V_0}{L} \\ V_0^* = \frac{i_L}{c} - \frac{\theta V_0}{c} \end{cases} \quad (2)$$

So, the state-space average model is

$$\begin{cases} \dot{i}_L^* = \frac{V_{in}}{L} - \frac{(1-u)}{L} V_0 \\ \dot{V}_0^* = \frac{(1-u)}{c} i_L - \frac{\theta V_0}{c} \end{cases} \quad (3)$$

where, $\theta = 1/R$, and u - duty cycle of the switch S, which fulfills $u [0, 1]$ - control input.

The V-I characteristics of a CPL are given by,

$$i_{CPL} = \frac{P_{CPL}}{v_{CPL}}, \quad (4)$$

where, v_{CPL} and i_{CPL} represents the instant values of input current, and voltage of the CPL, and P_{CPL} represents the power of CPL.

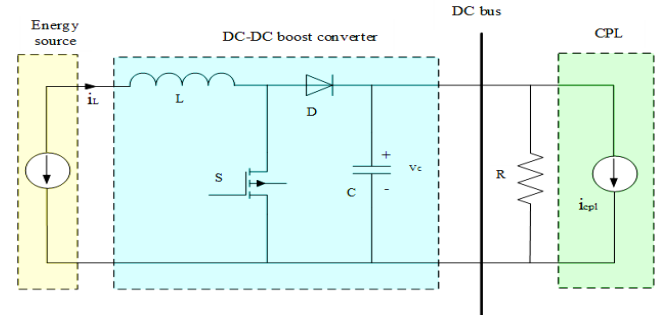


Fig. 1 – Design of proposed boost converter with CPL.

4. DESIGN OF PROPOSED AQO-DSM CONTROL STRATEGY

This section presents a novel Aquila optimization algorithm-based Discrete Sliding Mode (AQO-DSM) strategy for a CPL-enabled boost converter.

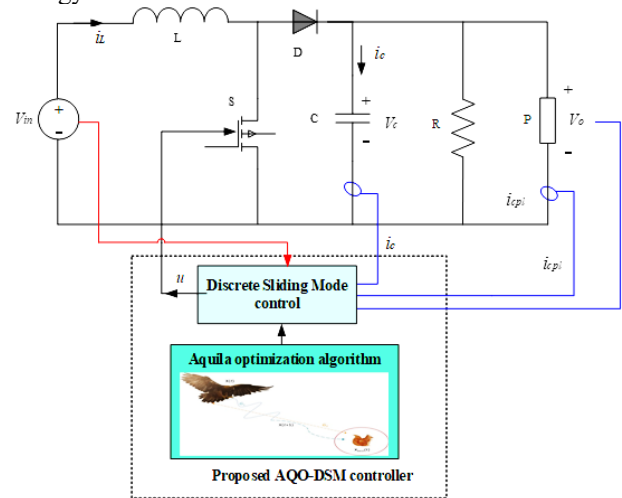


Fig. 2 – Proposed AQO-DSM controller-based converter with CPL.

A nonlinear control strategy is presented to ensure the system remains stable and responds quickly to large load and DC-bus voltage disturbances. This work aims to design converter controllers for DC-DC converters that can supply the required power while maintaining a sufficient level of

DC-bus voltage. If only one source is available to provide the off-grid mode microgrid, the CPLs of the DC-DC converters will determine the overall load in the MG. Figure 2 shows the proposed AQO-DSM controller-based converter with CPL.

4.1 PROPOSED AQO-DSM CONTROL STRATEGY

This paper uses the Aquila optimization algorithm (AQO) [24] to optimize the discrete sliding mode control. The Aquila optimization algorithm primarily relies on the control signal $u[k]$ and its derivatives $u[k+1]$ on establishing the pattern of Aquila's new position and shifting the search approach from exploration to exploitation. To construct the proposed AQO-DSM control, the following converter (source converter) calculations focus on the switch's OFF and ON states: Consider a nonlinear model with a single input and a single output.

$$\begin{cases} a(k+1) = f(a(k)), u(k) \\ b(k) = h(a(k)) \end{cases}, \quad (5)$$

where a is the state vector, $a \in M \subset R^a$ n -dimensional analytic manifold, u is – the control input, and b is – the system output.

A discrete SMC can be developed to fulfill the following r -order difference in the system output:

$$b(k+r) + \sum_{i=0}^{r-1} \lambda_i b(k+i) - b_{ref}(k) = 0, \quad (6)$$

where $b_{ref}(k)$ – desired reference output.

When the discrete sliding regime is reached, eq. (6) must be met. The invariance requirement can be used to identify this regime

$$\alpha(k+1) - \alpha(k) = 0.$$

The sliding surface can be obtained by identifying $\alpha(k+1) - \alpha(k)$ with eq. (6)

$$\alpha(k+1) - \alpha(k) = b(k+r) + \sum_{i=0}^{r-1} \lambda_i b(k+i) - b_{ref}(k) = 0 \quad (7)$$

where, α denotes the sliding surface. When the sliding surface specified in (7) is used, the system's dynamic behavior is:

$$\Phi_{j(k+r) + \sum_{i=0}^{r-1} \lambda_i \varphi_j(k+i) - b_{ref}(k+j-1) = 0. \quad (8)$$

λ_i represents the coefficients of sliding surface dynamics, φ is the dynamic behavior of the system on the sliding surface, b_{ref} is the desired reference output. For all $1 \leq j \leq r$, Observe that the stability of $\varphi_j(k)$ for $1 \leq j \leq r$ is guaranteed by the stability of the dynamics imposed on $b(k)$ in eq. (6). The boost converter's dynamic behavior is expressed below:

$$V_{ref}(kT) = V_{dc} + A \sin(2\pi f_0 kT), \quad (9)$$

$$\dot{a}(t) = Fa(t) + Ga(t)u(t) + p. \quad (10)$$

Using the forward difference approach, we can calculate:

$$a(kT+T) = Xa(kT) + Ya(kT)u(kT) + Z, \quad (11)$$

where $a(kT) = [i_L(kT), V_o(kT)]^T$ is the state vector, T -sampling period, $u(kT)$ denotes the control action at time kT , and the matrices X , Y , and Z are:

$$X = \begin{bmatrix} 1 & 0 \\ 0 & \left(1 - \frac{T}{RC}\right) \end{bmatrix}, Y = \begin{bmatrix} 0 & -T/L \\ T/L & 0 \end{bmatrix}, \text{ and } Z = \begin{bmatrix} ET/L \\ 0 \end{bmatrix}.$$

$u(kT)$ – control action is defined by:

$$u(kT) = \begin{cases} 0 & \text{when the switch is ON,} \\ 1 & \text{when the switch is OFF.} \end{cases}$$

In taking an output function as $\varphi_1(kT) = b(kT) = V_o(kT)$, accordingly, the dynamic imposition approach cannot be applied to the discretized system since its relative

degree, $r = 1$, equals 1.

By replacing the saturation function below with the following, the chattering phenomenon can be eliminated, and the sliding function $s_f(s, \varphi)$ is given by

$$s_f(s, \varphi) = \begin{cases} \frac{s}{\varphi} & \text{if } \left| \frac{s}{\varphi} \right| \leq 1 \\ \text{sign}(s) & \text{else} \end{cases} \quad (12)$$

where $\varphi > 0$ sliding manifold's boundary layer thickness.

4.2 ANALYSIS OF AQUILA OPTIMIZATION ALGORITHM (AQO)

To capture its prey, an AQO algorithm typically imitates the social behavior of a bird. Upgrading the current population of agents continues until the optimal solution is found by considering both the AQO and the best agent. There are N solutions that make up the initial population m .

$$Nm = s_1 * (ik_n - jk_n) + ij_n, m = 1, 2, 3 \dots x, N = 1, 2, \dots, Dim \quad (13)$$

Equation (12) uses the terms ik_n and jk_n to denote the search space boundaries. The random value $s_1 \in [0, 1]$ is indicated, and the agent's dimension is Dim . Afterward, until the ideal answer is found, the AQO approach proceeds with either exploration or exploitation [22]. Its mathematical formulation is as follows: the exploration uses the best agent (N_b) and the average of the agents (N_a):

$$Nm(t+1) = Na(t) * \left(\frac{1-t}{T}\right) + (Nb(t) - Na(t) * \text{rand}), \quad (14)$$

$$Nb(t) = \frac{1}{x} \sum_{i=1}^x z(t), \quad x = 1, 2, \dots, Dim. \quad (15)$$

Equation (15) governs the search throughout the exploration phase $\left(\frac{1-t}{T}\right)$. T represents the highest possible number of generations. In the exploration stage, the solutions are updated using the Levy flight (Levy(D) distribution) and to (Na). This is represented as:

$$Nm(t+1) = Na(t) * \text{Levy}(p) + Nr(t) + (u - v) * \text{rand}, \quad (16)$$

$$\text{Levy}(p) = d * \frac{v * \sigma}{|v|^\beta}, \quad \sigma = \left(\frac{f(1+\beta) * \sin\left(\frac{\pi\beta}{2}\right)}{f\left(\left(\frac{1+\beta}{2}\right) * \beta * 2\left(\frac{\beta-1}{2}\right)\right)} \right). \quad (17)$$

The parameters of the Levy flight distribution are represented by d, σ, β . Equation (17) uses u and v to represent the random values, where $d = 0.01$ and $\beta = 1.5$. Furthermore, as the equation below illustrates, H_1 and H_2 denotes the motions utilized to track the optimum individual solution:

$$H_1 = 2 * \text{rand}() - 1, H_2 = 2 * \left(\frac{1-t}{T}\right), \quad (18)$$

$$H_2 = 2 * \left(\frac{1-t}{T}\right). \quad (19)$$

4.3 STABILITY ANALYSIS

The proposed AQO-DSM controller aims to preserve the motion of the system parameters along the sliding surface. Therefore, there shouldn't be any discrepancies between the voltage used as a reference and the actual output voltage. This can be expressed as follows:

$$S_s = k_1(u_{oe} - u_o) = 0. \quad (20)$$

$$d(t) = 1 - \frac{u_i}{u_{oe}}. \quad (21)$$

where, u_{oe} is the desired output voltage, u_o actual output voltage.

The candidate Lyapunov function $V(x)$, according to Lyapunov's stability theorem, is:

$$V(x) = \frac{1}{2} e^T Q_e = \frac{1}{2} (x - x_e)^T Q (x - x_e), \quad (22)$$

where $x = [i_L \ u_0]^T$ are state variables, Q - diagonal matrix, e is the error vector $[a_1 \ 0; 0 \ a_2]$ ($a_1, a_2 > 0$) and markedly $V(i_e, u_e) = 0$.

Equation (22) yields

$$V(i_L, u_e) = \frac{1}{2}[a_1(i_L - i_e)^2 + a_2(u_0 - u_e)^2]. \quad (23)$$

Therefore, for any $x \neq x_e$, $V > 0$, and when $x = x_e$, $V = 0$. The derivative of eq. (21) is then examined:

$$\dot{V} = \frac{1}{2} \dot{e}^T Q_e + \frac{1}{2} e^T Q_e =$$

$$= -a_2 \frac{k_2}{k_1} (u_0 - u_e)^2 + \frac{a_2}{L} [u_i - (1 - S)u_0] \left[i_L - \frac{u_e^2}{Ru_i} \right]. \quad (24)$$

From the energy conservation law when $u_0 > u_e$, then $[u_i - (1 - S)u_0] < 0$. This leads to $i_L > i_e$, resulting in $[i_L - u_e^2/Ru_i] > 0$. Else when $u_0 < u_e$, then $[u_i - (1 - S)u_0] > 0$, giving $i_L < i_e$, which results in $[i_L - u_e^2/Ru_i] < 0$.

In summary, for any $x \neq x_e$ eq. (24) is negative and when $x = x_e$ eq. (24) is zero. Thus eq. (24) is negative definite. Based on the results of this analysis, a Lyapunov function is the candidate function, and the system is stable under Lyapunov conditions. As a result, the equilibrium points of the design are asymptotically stable.

5. RESULTS AND DISCUSSIONS

The performance of the proposed Aquila optimization algorithm-based discrete sliding mode (AQO-DSM) controller, which is meant to maintain system stability and enable fast response to large load and DC-bus voltage disturbances, is briefly described in this section for a DC-DC boost converter with CPL-enabled. The proposed model with variable loads, as seen in Figure 3, is investigated using a MATLAB program. Table 1 presents the parameters used in the simulation parameter of the suggested controller.

Table 1

System simulation parameters.

Sl. No	Parameters	Specifications
1.	Capacitance, C	0.47 mF
2.	Switching frequency, f_s	20 kHz
3.	DC bus voltage reference	50 V
4.	Inductance, L	1 mH
5.	Converter input voltage, V_{in}	25 V

5.1 SIMULATION RESULTS

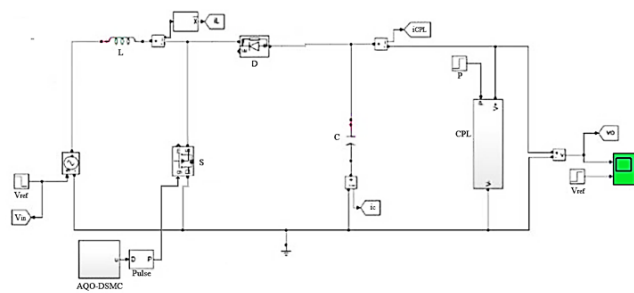


Fig.3 – Proposed Simulink model of the converter with CPL.

Two simulation tests, a CPL variation test, and an input voltage variation test, yield simulated results.

5.1.1 CPL VARIATION TEST

In Figure 4, the voltages and currents are shown as a function of the variation of CPL at time = 0.2 s from 100 W to 160 W and at time = 0.4 s from 160 W to 100 W. The output voltage is consistently accurate and constant at 50 V, even when there are significant variations in CPL.

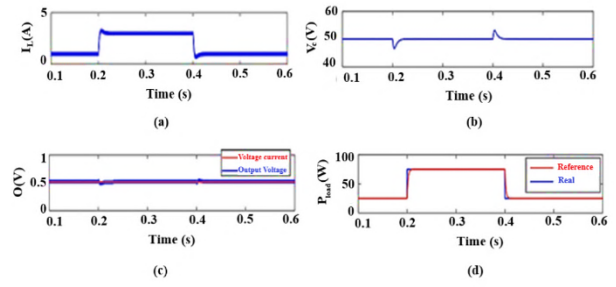


Fig. 4 – Simulation results with CPL variation of (a) Inductor current (b) Capacitance voltage (c) Output voltage (d) Load power.

5.1.2 INPUT VOLTAGE VARIATION TEST

An output voltage control test is provided to assess whether the control works when the input voltage changes. Figure 5 illustrates that the system reacts to DC bus voltage variations when operating in pure CPL circumstances. During heavy load conditions, 160 W is applied to the CPL. Time = 0.2 s creates a voltage reference change from 50 V to 45 V, and time = 0.4 s creates a voltage reference change from 45 V to 55 V. The duty ratio changes from 0.5 to 0.445 after the change of reference value, which indicates bus voltage that follows its reference value within 10ms after the change.

This is despite the adverse effects of CPL on the reference voltage. The error in the V_{out} is less than 0.1 V. The reference voltage is captured within lower than 4 ms. At steady-state error, the current of CPL ranges lower than 0.001 A. The steady-state error and overshoot, on the other hand, are decreasing. Because these modifications were so few, they did not lead to instability.

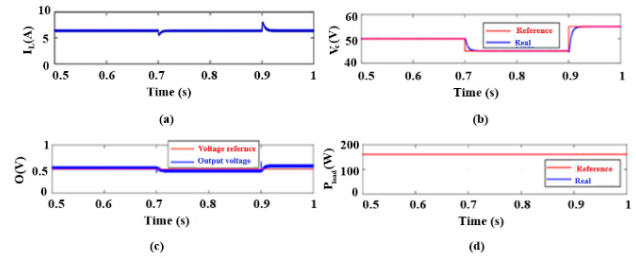


Fig. 5 – Simulation results with input voltage variation (a) Inductor current (b) Capacitance voltage (c) Output voltage (d) load power.

5.2 EXPERIMENTAL RESULTS

The experimental setup shown in Fig. 6 uses a DC source, DC/DC boost converter, resistive load (R load), and CPL to test the efficacy of the proposed AQO-DSM controller. A load-side converter supplies a resistive load with a precisely controlled output voltage. A resistance load regulates the load demand of the CPL. First, a variation of CPL is tested, and second, the input voltage variation is evaluated in experimental results.

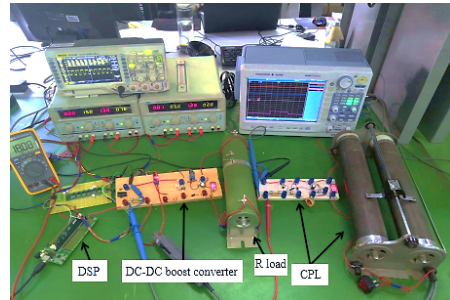


Fig. 6 – Proposed experimental setup.

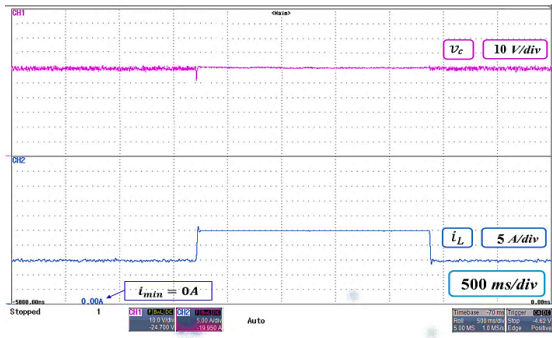


Fig. 7 – Experiment result of proposed AQO-DSM controller for CPL variation.

As shown in Fig. 7, the output voltage, input voltage, and inductor current show dynamic responses when the resistive load has been removed. Initially, 100 W is set as the load. After that, CPL increases up to 160 W under heavy load conditions. When the output voltage at 50 V reaches its reference value of 40 ms, it is indicated that the system is stable.

Figure 8 illustrates the impact of input voltage variation. There is a constant load of 50W. Inductor current increases as the V_{in} decreases from 25 V to 20 V, but the V_{out} remains at 50 V with no noticeable disturbance. Thus, the suggested method ensures stable operation even when the input voltage varies.

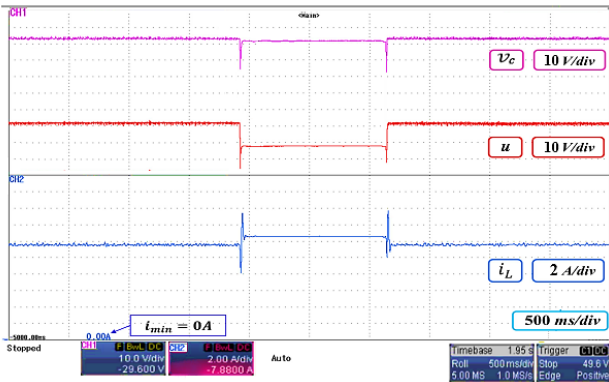


Fig. 8 – Experiment result of proposed AQO-DSM controller for input voltage variation.

5.3 PERFORMANCE COMPARISON ANALYSIS

The suggested controller's benefits are illustrated by comparing it with other controllers currently in use for the boost converter with CPL and input voltage variations, including conventional Sliding Mode Control (SMC), interval type-2 fuzzy sliding mode control (F-SMC), and Super Twisting Algorithm (STA)-based SMC (STA-SMC). Tables 2 and 3 show the performance comparison of the proposed and state-of-the-art controllers at CPL variation and input voltage variation.

Table 2
Performance comparison of CPL variation.

CPL variation ($P_{CPL} = 160$ W to 100W), $V_{ref} = 50$ V								
Param.	Controllers							
	SMC		F-SMC		STA-SMC		Proposed AQO-DSMC	
	Simlu	Expe.	Simlu	Expe.	Simlu	Expe.	Simlu	Expe.
Settling (s)	3.63	3.66	0.72	0.74	0.003	0.0045	0.0009	0.0012
Rise time	5.72	5.75	2.87	2.88	0.023	0.025	0.001	0.0015
Overshoot (%)	4.501	4.506	0.55	0.54	0.32	0.35	0.018	0.02
Steady-st error (%)	1.72	1.76	0.005	0.006	0.0079	0.0078	≈ 0	≈ 0

Table 3

Performance comparison of CPL variation.

Input voltage variation ($V_{ref} = 50$ V – 45 V), $P_{CPL} = 160$ W								
Param.	Controllers							
	SMC		F-SMC		STA-SMC		Proposed AQO-DSMC	
	Simlu	Expe	Simlu	Exp	Simlu	Expe.	Simlu	Expe.
Settling (s)	2.55	2.54	0.51	0.55	0.0028	0.0031	0.0004	0.0052
Rise time	3.67	3.69	2.74	2.75	0.063	0.65	0.001	0.0013
Overshod (%)	4.213	4.215	0.86	0.85	0.01	0.016	0.011	0.01
Steady-st error (%)	1.59	1.61	0.006	0.0065	0.0052	0.0051	≈ 0	≈ 0

Considering the above results, the suggested controller provides quick dynamic performance and system stability. The experimental scenarios' dynamic responsiveness is slightly slower than the simulated findings. The programmable controller bandwidth limits the variance of the constant power demand throughout the experimental testing, as opposed to the optimal constant power load with a step change. Table 2 shows a decrease in CPL power, deterioration of the controller's dynamic response, and a decrease in settling-rising times of about 0.009 s in simulation and 0.0012 s in experimental results compared to existing controllers. Table 3 shows the dynamic responses of the controller at various input voltages. These mistakes and malfunctions are too little to impact system performance.

6. CONCLUSION

An analysis of DC microgrid instability is presented in this study due to the occurrence of constant power loads. Aquila optimization-based discrete sliding mode (AQO-DSM) controller-based DC-DC boost converter. The proposed methodology's effectiveness has been assessed using simulation and experimental validation. The suggested model is simulated using a MATLAB program to evaluate the controller's performance by altering the loads. This proposed AQO-DSM controller maintains a steady state with a constant output voltage despite variations in continuous Load power and input voltage. The proposed controller's performance is compared to the existing controllers. The stability analysis and simulated results conclude that the proposed AQO-DSM controller is easy to implement, its dynamic response is fast, its overshoot is slight under loaded conditions, a consistent reduction in chatter, and its robustness is greater than that of existing controllers. An adaptive nonlinear composite controller with parametric uncertainty and external disturbances will be designed in the future.

ACKNOWLEDGMENTS

The author would like to express his heartfelt gratitude to the supervisor for his guidance and unwavering support during this research as well as his advice and support.

Received on 18 May 2023

REFERENCES

1. Y. Zhang, W. Wei, *Decentralized coordination control strategy of the PV generator, storage battery and hydrogen production unit in islanded AC microgrid*, IET Renewable Power Generation, **14**, 6, pp. 1053–1062 (2020).
2. A.A. Memon, K. Kauhaniemi, *A critical review of AC Microgrid protection issues and available solutions*, Electric Power Systems Research, **129**, pp. 23–31 (2015).
3. Y. Li, K.R. Vannorsdel, A.J. Zirger, M. Norris, D. Maksimovic, *Current*

- mode control for boost converters with constant power loads*, IEEE Transactions on Circuits and Systems I: Regular Papers, **59**, 1, pp. 198–206 (2011).
4. D.S. Dakshina, Della Reasa Valiaveetil, A. Bindhu, *Alzheimer disease detection via deep learning-based shuffle network*, International Journal of Current Bio-Medical Engineering, **01**, 01, pp. 09–15, (2023).
 5. M. Wang, F. Tang, X. Wu, J. Niu, Y. Zhang, J. Wang, *A nonlinear control strategy for DC-DC converter with unknown constant power load using damping and interconnection injecting*, Energies, **14**, 11, p. 3031 (2021).
 6. X. Lu, K. Sun, J.M. Guerrero, J.C. Vasquez, L. Huang, J. Wang, *Stability enhancement based on virtual impedance for DC microgrids with constant power loads*, IEEE Transactions on Smart Grid, **6**, 6, pp. 2770–2783 (2015).
 7. Q. Xu, C. Zhang, C. Wen, P. Wang, *A novel composite nonlinear controller for stabilization of constant power load in DC microgrid*, IEEE Transactions on Smart Grid, **10**, 1, pp. 752–761 (2017).
 8. P. Deepa, S. Rajakumar, P.J. Shermila, E.A. Devi, M.E. Prince, A.J.G. Malar, *New hybrid Cuk-Landsman high gain dc-dc converter modelling and analysis*, Power, **9**, 8, 8–16 (2022).
 9. Y. Zhao, W. Qiao, D. Ha, *A sliding-mode duty-ratio controller for DC/DC buck converters with constant power loads*, IEEE Transactions on Industry Applications, **50**, 2, pp. 1448–1458 (2013).
 10. N. Vafamand, S. Yousefizadeh, M.H. Khooban, J.D. Bendtsen, T. Dragičević, *Adaptive TS fuzzy-based MPC for DC microgrids with dynamic CPLs: nonlinear power observer approach*, IEEE Systems Journal, **13**, 3, pp. 3203–3210 (2018).
 11. K.E.L. Marcillo, D.A.P. Guingla, W. Barra, R.L.P. De Medeiros, E.M. Rocha, D.A.V. Benavides, F.G. Nogueira, *Interval robust controller to minimize oscillations effects caused by constant power load in a DC multi-converter buck-buck system*, IEEE Access, **b**, pp. 26324–26342 (2019).
 12. J. Wu, Y. Lu, *Adaptive backstepping sliding mode control for boost converter with constant power load*, IEEE Access, **7**, pp. 50797–50807 (2019).
 13. J. Wang, W. Luo, J. Liu, L. Wu, *Adaptive type-2 FNN-based dynamic sliding mode control of DC-DC boost converters*, IEEE Transactions on systems, man, and cybernetics: systems, **51**, 4, pp. 2246–2257 (2019).
 14. S. Pang, B. Nahid-Mobarakeh, S. Pierfederici, Y. Huangfu, G. Luo, F. Gao, *Toward stabilization of constant power loads using IDA-PBC for cascaded LC filter DC/DC converters*, IEEE Journal of Emerging and Selected Topics in Power Electronics, **9**, 2, pp. 1302–1314 (2019).
 15. W. He, R. Ortega, *Design and implementation of adaptive energy shaping control for DC-DC converters with constant power loads*, IEEE Transactions on Industrial Informatics, **16**, 8, pp. 5053–5064 (2019).
 16. Q. Xu, Y. Xu, C. Zhang, P. Wang, *A robust droop-based autonomous controller for decentralized power sharing in DC microgrid considering large-signal stability*, IEEE Transactions on Industrial Informatics, **16**, 3, pp. 1483–1494 (2019).
 17. M. Boukerdja, A. Chouder, L. Hassaine, B. O. Bouamama, W. Issa, K. Louassaa, *H_∞ based control of a DC/DC buck converter feeding a constant power load in uncertain DC microgrid system*, ISA transactions, **105**, pp. 278–295 (2020).
 18. A. Azizi, M. Hamzeh, *Stability analysis of a DC microgrid with constant power loads using small-signal equivalent circuit*, In 2020 11th Power Electronics, Drive Systems, and Technologies Conference (PEDSTC), IEEE, pp. 1–6 (2020).
 19. O. Kaplan, F. Bodur, *Super twisting algorithm based sliding mode controller for buck converter with constant power load*, In 2021 9th International Conference on Smart Grid (icSmartGrid), pp. 137–142 (2021).
 20. T.K. Nizami, A. Chakravarty, C. Mahanta, A. Iqbal, A. Hosseinpour, *Enhanced dynamic performance in DC-DC converter-PMDC motor combination through an intelligent non-linear adaptive control scheme*, IET Power Electronics (2022).
 21. M.K. Al-Nussairi, R. Bayindir, *DC-dc boost converter stability with constant power load*, In 2018 IEEE 18th International Power Electronics and Motion Control Conference (PEMC), IEEE, pp. 1061–1066 (2018).
 22. L. Abualigah, D. Yousri, M. Abd Elaziz, A.A. Ewees, M.A. Al-Qaness, A.H. Gandomi, *AAquila optimizer: a novel meta-heuristic optimization algorithm*, Computers & Industrial Engineering, **157**, pp. 107250 (2021).
 23. T.H. Van, T. Le Van, T.M.N. Thi, M.Q. Duong, G.N. Sava, *Improving the output of DC-DC converter by phase shift full bridge applied to renewable energy*, Rev. Roum. Sci. Techn. – Électrotechn. Et Énerg., **66**, 3, pp. 175–180 (2021).
 24. A. Bogza, D. Florica, *The parallel connection of phase-shifted full-bridge DC-DC converters*, Rev. Roum. Sci. Techn. – Électrotechn. Et Énerg., **65**, 4, pp. 229–234 (2021).
 25. M. Ramya Devi, K.V. Sreelekha, R. Jayaraj, *Jarrot butterfly optimized Flamingo search algorithm for optimal routing in WSN*, International Journal of Data Science and Artificial Intelligence, **02**, 2, pp. 48–54, (2024).
 26. T. Kavitha, N. Pandeewari, R. Shobana, V.R. Vinothini, K. Sakthisudhan, A. Jeyam, A.J.G. Malar, *Data congestion control framework in wireless sensor network in IoT enabled intelligent transportation system*, Measurement: Sensors, **24**, pp. 100563 (2022).